Article

Folding Induced Assembly of Polypeptide Decorated Gold Nanoparticles

Daniel Aili, Karin Enander, Johan Rydberg, Irina Nesterenko, Fredrik Björefors, Lars Baltzer, and Bo Liedberg

J. Am. Chem. Soc., **2008**, 130 (17), 5780-5788 • DOI: 10.1021/ja711330f • Publication Date (Web): 02 April 2008

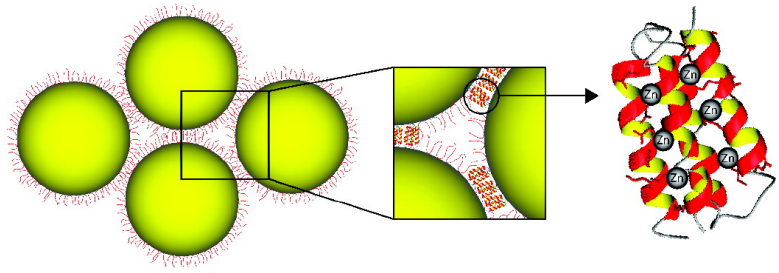

J|A|C|S
ARTICLES

Published on Web 04/02/2008

Folding Induced Assembly of Polypeptide Decorated Gold Nanoparticles

Daniel Aili,[†] Karin Enander,[†] Johan Rydberg,[‡] Irina Nesterenko,[†] Fredrik Björefors,[†] Lars Baltzer,[‡] and Bo Liedberg[†,*]

Division of Sensor Science and Molecular Physics, Department of Physics, Chemistry and Biology, Linköping University, SE-581 83 Linköping, Sweden, and Division of Organic Chemistry, Department of Biochemistry and Organic Chemistry, BMC, Box 599, Uppsala University, SE-751 24 Uppsala, Sweden

Received December 21, 2007; E-mail: bol@ifm.liu.se

Abstract: Reversible assembly of gold nanoparticles controlled by the homodimerization and folding of an immobilized *de novo* designed synthetic polypeptide is described. In solution at neutral pH, the polypeptide folds into a helix–loop–helix four-helix bundle in the presence of zinc ions. When immobilized on gold nanoparticles, the addition of zinc ions induces dimerization and folding between peptide monomers located on separate particles, resulting in rapid particle aggregation. The particles can be completely redispersed by removal of the zinc ions from the peptide upon addition of EDTA. Calcium ions, which do not induce folding in solution, have no effect on the stability of the peptide decorated particles. The contribution from folding on particle assembly was further determined utilizing a reference peptide with the same primary sequence but containing both D and L amino acids. Particles functionalized with the reference peptide do not aggregate, as the peptides are unable to fold. The two peptides, linked to the nanoparticle surface via a cysteine residue located in the loop region, form submonolayers on planar gold with comparable properties regarding surface density, orientation, and ability to interact with zinc ions. These results demonstrate that nanoparticle assembly can be induced, controlled, and to some extent tuned, by exploiting specific molecular interactions involved in polypeptide folding.

Introduction

Composite materials and devices based on a combination of metal nanoparticles and biomolecular building blocks are highly interesting for the development of novel sensors[1–5] and for applications and fundamental studies within plasmonics.[6,7] Although in recent years an increasing number of application areas for these materials have been identified, there is a long tradition in using metal nanoparticles together with a range of biologically relevant molecules for various purposes. The use of antibody conjugated gold nanoparticles has, e.g., been widely employed for immunohistochemical labeling[8] and in a large number of rapid colorimetric bioanalytical assays intended for point-of-care applications.[9,10] Mirkin et al.[11,12] have shown how ssDNA functionalized gold nanoparticles can be used for the detection of single base pair mismatches as well as for controlling nanoparticle assembly. In addition, gold nanoparticles have been employed as a detector and modulator of conformational changes of both natural proteins[13,14] and synthetic polypeptides.[15,16] Interactions between immobilized designed coiled-coil polypeptide motifs have also been utilized for the assembly of gold nanoparticles.[15,17]

Thiolated DNA is a suitable molecule for surface functionalization of gold nanoparticles, mainly due to its high molecular net charge that provides effective electrostatic stabilization of the particles, as well as to its predictable interactions with complementary target DNA. Proteins with these properties are more difficult to identify. Recent advances in the development of synthetic *de novo* designed polypeptides, however, have resulted in a number of interesting scaffolds with versatile structures and chemical properties suitable for nanoparticle

[†] Linköping University.
[‡] Uppsala University.

(1) Thanh, N. T. K.; Rosenzweig, Z. *Anal. Chem.* **2002**, *74*, 1624–1628.
(2) Xu, X. Y.; Han, M. S.; Mirkin, C. A. *Angew. Chem., Int. Ed.* **2007**, *46*, 3468–3470.
(3) Lee, J. S.; Han, M. S.; Mirkin, C. A. *Angew. Chem., Int. Ed.* **2007**, *46*, 4093–4096.
(4) Schultz, D. A. *Curr. Opin. Biotechnol.* **2003**, *14*, 13–22.
(5) Aili, D.; Enander, K.; Baltzer, L.; Liedberg, B. *Biochem. Soc. Trans.* **2007**, *35*, 532–534.
(6) Ozbay, E. *Science* **2006**, *311*, 189–193.
(7) Aslan, K.; Gryczynski, I.; Malicka, J.; Matveeva, E.; Lakowicz, J. R.; Geddes, C. D. *Curr. Opin. Biotechnol.* **2005**, *16*, 55–62.
(8) Faulk, W. P.; Taylor, G. M. *Immunochemistry* **1971**, *8*, 1081–1083.
(9) Niemeyer, C. M. *Angew. Chem., Int. Ed.* **2001**, *40*, 4128–4158.
(10) Daniel, M. C.; Astruc, D. *Chem. Rev.* **2004**, *104*, 293–346.
(11) Mirkin, C. A.; Letsinger, R. L.; Mucic, R. C.; Storhoff, J. J. *Nature* **1996**, *382*, 607–609.
(12) Elghanian, R.; Storhoff, J. J.; Mucic, R. C.; Letsinger, R. L.; Mirkin, C. A. *Science* **1997**, *277*, 1078–1081.
(13) Chah, S.; Hammond, M. R.; Zare, R. N. *Chem. Biol.* **2005**, *12*, 323–328.
(14) Verma, A.; Srivastava, S.; Rotello, V. M. *Chem. Mater.* **2005**, *17*, 6317–6322.
(15) Stevens, M. M.; Flynn, N. T.; Wang, C.; Tirrell, D. A.; Langer, R. *Adv. Mater.* **2004**, *16*, 915–918.
(16) Aili, D.; Enander, K.; Rydberg, J.; Lundstrom, I.; Baltzer, L.; Liedberg, B. *J. Am. Chem. Soc.* **2006**, *128*, 2194–2195.
(17) Ryadnov, M. G.; Ceyhan, B.; Niemeyer, C. M.; Woolfson, D. N. *J. Am. Chem. Soc.* **2003**, *125*, 9388–9394.

10.1021/ja711330f CCC: $40.75

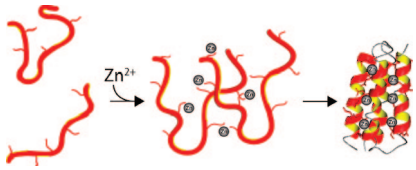

Figure 1. In the presence of Zn^{2+} the designed polypeptide JR2E dimerizes and folds into a four-helix bundle.

surface functionalization.[16,18] These designed polypeptides not only possess controllable structural properties but also enable introduction of catalytic groups as well as specific recognition,[19,20] which is highly interesting for engineering and design of new types of functional hybrid and composite materials.

Folding and function of many proteins are dependent on interactions with metal ions.[21,22] Zinc ions are, for example, a crucial component in a large family of DNA binding proteins and have a major impact on their three-dimensional structure and their potential to bind to DNA.[23] Metal ion interactions have also been utilized to induce folding and to stabilize the folded state of *de novo* designed polypeptides.[24–26] Kohn et al.[25] have described the successful design of a synthetic coiled-coil peptide that undergoes a transition from random coil to α-helical at pH 7 upon binding zinc ions to γ-carboxyglutamic acid residues located in g and e positions in the heptad repeat.

In this paper we present how the coordination of Zn^{2+} to a *de novo* designed polypeptide can induce dimerization and folding of the peptide, as schematically described in Figure 1. The folding event has further been utilized to induce a reversible assembly of peptide functionalized gold nanoparticles. The design of the polypeptides was based on the SA-42 motif,[27,28] a 42-residue *de novo* designed helix–loop–helix polypeptide that folds into a molten globule-like four-helix bundle upon dimerization but that is modified to allow for dimerization and folding only at a slightly acidic pH (pH < 6) or in the presence of selected metal ions. In order to describe and isolate the contribution from folding on the nanoparticle assembly, a designed reference peptide without the ability to fold was utilized. The peptide−metal ion interactions were examined both in solution and when the peptides were immobilized on planar gold surfaces as well as on gold nanoparticles. The present study is a continuation of previous work[16] where charge neutralization of immobilized peptides at an acidic pH was used to reversibly aggregate gold nanoparticles which in turn induced folding of the peptides. The advantage with the present approach is that we can induce folding and thereby nanoparticle assembly at a biologically relevant pH, and importantly, in this approach folding is the driving force for, and not the consequence of, nanoparticle assembly. Utilizing controlled polypeptide folding to induce nanoparticle assembly provides a novel and specific route for the design and construction of nanoarchitectures and complex composite materials for plasmonics and biosensor applications.

Experimental Section

Peptide Synthesis. The polypeptides JR2E (NAADLEKAIEALEKHLEAKGPVDAAQLEKQLEQAFEAFERAG), JR2EC, and JR2ECref were synthesized on a Pioneer automated peptide synthesizer (Applied Biosystems) using standard fluorenylmethoxycarbonyl (Fmoc) chemistry with *O*-(7-benzotriazole-1-yl)-1,1,3,3-tetramethyluronium tetrafluoroborate (TBTU, Alexis Biochemicals) as the activating reagent. The synthesis was performed on a 0.1 mmol scale with an Fmoc-Gly PEG-PS resin, and a 4-fold excess of amino acid was used in each coupling. The side chains of the amino acids (Calbiochem-Novabiochem AG) were protected by base-stable groups: *tert*-butyl ester (Asp, Glu), *tert*-butoxycarbonyl (Lys), trityl (His, Asn, Gln, Cys), and 2,2,4,6,7-pentamethyldihydrobenzofurane-5-sulfonyl (Arg). For JR2E and JR2EC only L-amino acids were used. For JR2ECref D-alanines were used throughout, while all other amino acids were in the L-form. Cys-containing peptides were cleaved from the resin by treatment with a mixture of trifluoroacetic acid (TFA), ethanedithiol, water, and triisopropylsilane (94:2.5:2.5:1 v/v; 15 mL per g of polymer) for 2 h at room temperature. JR2E was cleaved from the resin by treatment with a mixture of TFA, water, and triisopropylsilane (95:2.5:2.5 v/v; 15 mL per g of polymer) for 2 h at room temperature. After filtration, TFA was evaporated, and the peptides were precipitated by the addition of cold diethyl ether, centrifuged, resuspended in diethyl ether, and lyophilized. The crude products were purified by reversed-phase HPLC on a semipreparative HICHROM C-8 column. JR2E, JR2EC, and JR2ECref were eluted with a 30 min gradient of aqueous 2-propanol (JR2E: 35–36%; JR2EC: 30–50%; JR2ECref: 25–35%) in the presence of 0.1% TFA. The purified peptides were identified by MALDI-TOF mass spectrometry. The concentration of the polypeptides when dissolved was estimated under the assumption that they contained 25% water in the lyophilized state.

Nanoparticle Synthesis. Gold nanoparticles with an approximate average diameter of ∼13 nm were prepared by citrate reduction of $HAuCl_4$. All glassware was cleaned in a TL1 mixture consisting of 5/7 H_20, 1/7 H_20_2 (30%), and 1/7 NH_3 (25%) at ∼85 °C for at least 20 min and thoroughly rinsed with MilliQ water (18.2 MΩ cm) before use. 50 mL of an aqueous solution of 1 mM $HAuCl_4$ were brought to a reflux while stirring. 5 mL of 38.8 mM trisodium citrate were added rapidly, and the solution was refluxed for an additional 15 min while stirring vigorously. The color changed from pale yellow to deep red, and the suspension was thereafter allowed to cool to room temperature. The UV–vis spectra showed a sharp and characteristic plasmon band with a maximum at 518–520 nm. The size and monodispersity of the nanoparticles were determined using electron microscopy.

Peptide Immobilization on Planar Gold. Gold substrates for infrared reflection–absorption spectroscopy and ellipsometry were prepared by evaporating a 25 Å Ti adhesion layer followed by 2000 Å of Au on clean (111) silicon wafers in a Baltzers UMS 500 P system. The base pressure was below 10^{-9} Torr, and the evaporation pressure, on the low 10^{-7} Torr scale. Gold substrates for electrochemical impedance spectroscopy, 2000 Å Au on glass, were obtained from Biacore AB (Uppsala, Sweden). Prior to assembly, the gold substrates were cleaned in TL1 solution and carefully rinsed in MilliQ water. Immediately after cleaning, the substrates were immersed in a 20 μM peptide solution in 30 mM Bis-Tris at pH 7.0 and incubated for at least 18 h. Immediately before analysis, all surfaces were rinsed in MilliQ water, sonicated for 3 min, and dried under a stream of nitrogen. For studies of Zn^{2+} binding to peptide monomers, the sonicated peptide surfaces were incubated in a 10 mM Zn^{2+} solution at pH 7.0 for 60 min. Before measurement they were quickly rinsed in MilliQ water and dried.

(18) Nilsson, K. P. R.; Rydberg, J.; Baltzer, L.; Inganas, O. *Proc. Natl. Acad. Sci. U.S.A.* **2003**, *100*, 10170–10174.
(19) Enander, K.; Dolphin, G. T.; Andersson, L. K.; Liedberg, B.; Lundstrom, I.; Baltzer, L. *J. Org. Chem.* **2002**, *67*, 3120–3123.
(20) Enander, K.; Dolphin, G. T.; Baltzer, L. *J. Am. Chem. Soc.* **2004**, *126*, 4464–4465.
(21) Berg, J. M. *J. Biol. Chem.* **1990**, *265*, 6513–6516.
(22) Vallee, B. L.; Auld, D. S. *Biochemistry* **1990**, *29*, 5647–5659.
(23) Schwabe, J. W. R.; Klug, A. *Nat. Struct. Biol.* **1994**, *1*, 345–349.
(24) Nicoll, A. J.; Miller, D. J.; Futterer, K.; Ravelli, R.; Allemann, R. K. *J. Am. Chem. Soc.* **2006**, *128*, 9187–9193.
(25) Kohn, W. D.; Kay, C. M.; Sykes, B. D.; Hodges, R. S. *J. Am. Chem. Soc.* **1998**, *120*, 1124–1132.
(26) Ghosh, D.; Pecoraro, V. L. *Inorg. Chem.* **2004**, *43*, 7902–7915.
(27) Olofsson, S.; Johansson, G.; Baltzer, L. *J. Chem. Soc. Perk. T. 2* **1995**, *2047*, 2056.
(28) Olofsson, S.; Baltzer, L. *Fold. Des.* **1996**, *1*, 347–356.

Peptide Functionalization of Gold Nanoparticles. A 200 μM peptide solution in 10 mM citric buffer at pH 6.0 was mixed in a 1:1 ratio with the as-prepared gold nanoparticles (~10 nM) and incubated overnight. To remove unbound peptides remaining in solution, the particles were repeatedly centrifugated (~18 000 g) and the supernatant was removed and replaced with fresh 30 mM Bis-Tris buffer pH 7.0 until the resulting concentration of peptides in solution was less than 0.5 nM.

Structural Analysis in Solution Using CD Spectroscopy. Circular dichroism spectra were recorded with a CD6 spectrodichrograph (JobinYvon-Spex) using a 0.1 mm cuvette at room temperature. Each spectrum was collected as an average of three scans in the range 190–260 nm. The helical content was determined as the mean residue ellipticity at 222 nm, [Θ_{222}], and was calculated from

$$[\Theta]_{222} = \frac{\Theta_{222}^{obs} \cdot \mathrm{mrw}}{10 \cdot l \cdot c} \quad (1)$$

where Θ_{222}^{obs} is the observed ellipticity at 222 nm (deg), mrw is the mean residue weight (g/mol), c is the peptide concentration (g/mL), and l is the optical path length of the cell (cm).

Infrared Reflection–Absorption Spectroscopy. RA spectra were recorded using a Bruker IFS 66 system, equipped with a liquid nitrogen cooled mercury cadmium telluride (MCT) detector and a grazing angle (85°) infrared reflection accessory. The measurement chamber was continuously purged with nitrogen gas during the measurements to reduce the amount of interfering water. 3000 scans were collected at a resolution of 2 cm^{-1}. Before Fourier transformation a three-term Blackmann−Harris apodization function was applied to the interferrograms. Deuterated hexadecanthiol ($HS(CD_2)_{15}CD_3$) immobilized on gold was used as a reference to record the background spectrum.

Transmission FT-IR Spectroscopy. IR spectra of peptides immobilized on gold nanoparticles were recorded using a Bruker IFS 48 system. The measurement chamber was evacuated to a pressure of 10^{-2} mbar during the measurements to reduce the amount of interfering water. 200 scans were collected at a resolution of 2 cm^{-1}. Before Fourier transformation, a three-term Blackmann−Harris apodization function was applied to the interferrograms. The peptide-modified particles were dispersed in MilliQ water and dried on a CaF_2 window using nitrogen.

Null Ellipsometry. Null-ellipsometric measurements were conducted on an automatic Rudolph Research AutoEL III ellipsometer with a He−Ne laser light source operating at 632.8 nm at an angle of incidence of 70°. An optical model based on isotropic optical constants for the peptide layer $N_{pep} = n + ik = 1.50$, with n = refractive index and k = extinction coefficient, was used for the evaluation of the film thickness. Results from at least five spots on each surface were averaged.

UV–vis Spectroscopy. UV–vis spectroscopy was performed on a Schimadzu UV-1601PC spectrophotometer with 0.5 nm resolution at room temperature.

TEM. TEM was conducted on a Philips CM20 Ultra-Twin lens high-resolution microscope operating at 200 kV. 20 μL of the samples were incubated on carbon coated TEM grids for 2 min before the suspension was removed using filter paper. The grids were dried before analysis.

Results and Discussion

Polypeptide Design and Synthesis. JR2E and JR2EC are glutamic acid rich 42-mer polypeptides that are able to fold into homodimers of amphiphilic helix–loop–helix motifs. The design of JR2E and JR2EC was based upon the SA-42 motif.[27,28] At neutral pH, the peptides have a net charge of –5, which prevents dimerization and folding.[18] When lowering the pH, glutamic acid residues in the peptides are gradually protonated, which reduces the net charge and allows for dimerization to occur. This process is primarily driven by the formation of a hydrophobic core made up by the hydrophobic faces of the amphiphilic helices. JR2EC differs from JR2E in that it has a Cys in position 22 instead of a Val, located in the loop region, to enable site-specific thiol dependent immobilization on gold substrates. Position 22 was chosen to minimize the risk of disabling helix formation upon immobilization. The thiol group of Cys is often involved in metal ion binding in natural proteins but is not accessible for interactions in JR2EC when the peptide is immobilized. To be able to directly compare metal ion interactions between surface bound JR2EC and peptides in solution, JR2E was employed for the solution studies. In order to investigate the impact of folding on particle aggregation, an additional peptide, JR2ECref, with the same primary sequence as that for JR2EC with the exception that all L-Ala residues were exchanged by D-Ala, was also synthesized. The incorporation of D-amino acids prevents the polypeptide from folding under any circumstances. The peptides were synthesized on the solid phase and cleaved from the resin by 95% trifluoroacetic acid, purified by reversed-phase HPLC, and identified from their matrix-assisted laser desorption/ionization time-of-flight (MALDI-TOF) spectra.

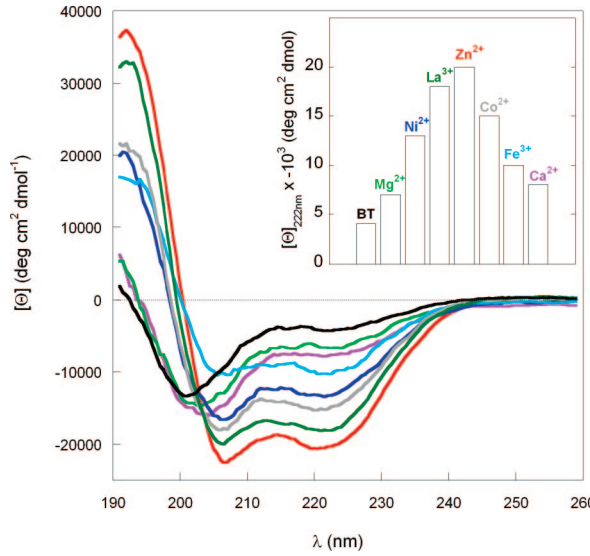

Figure 2. CD spectra of 200 μM JR2E at pH 7 in the presence of 10 mM of metal salts: (red) Zn^{2+}, (green) La^{3+}, (gray) Co^{2+}, (blue) Ni^{2+}, (light blue) Fe^{3+}, (purple) Ca^{2+}, (light green) Mg^{2+}, and (black) buffer only. Inset: Mean residue ellipticity at 222 nm ($\times -10^3$) in the presence of 10 mM metal salt pH 7. BT is the mean residue ellipticity of JR2E in 30 mM Bis-Tris pH 7.

Dimerization and Folding in Solution. The secondary structure of the polypeptides in solution was studied using circular dichroism (CD) spectroscopy. As reported previously,[16] JR2ECref does not fold at any pH. JR2EC and JR2E have no ordered secondary structure at pH 7 but dimerize and fold into molten globule-like four-helix bundles below pH 6.[16] CD spectroscopy did not reveal any significant differences in secondary structure between JR2E and JR2EC at neither neutral nor acidic pH or in the presence of Zn^{2+}.

The ability of metal ions to coordinate to certain amino acids allows for metal ion induced folding of JR2E (Figure 2). The largest folding tendency was seen upon addition of Zn^{2+}. In the presence of 10 mM $ZnCl_2$ at pH 7.0, a mean residue ellipticity of $[\Theta]_{222} = -19500 \pm 1000$ deg cm^2 $dmol^{-1}$ was obtained for JR2E (0.20 mM), corresponding to a molar fraction of folded peptide (f_f) of approximately 95%, where $f_f = ([\Theta]_{222} - [\Theta]_{222unfolded})/([\Theta]_{222folded} - [\Theta]_{222unfolded})$

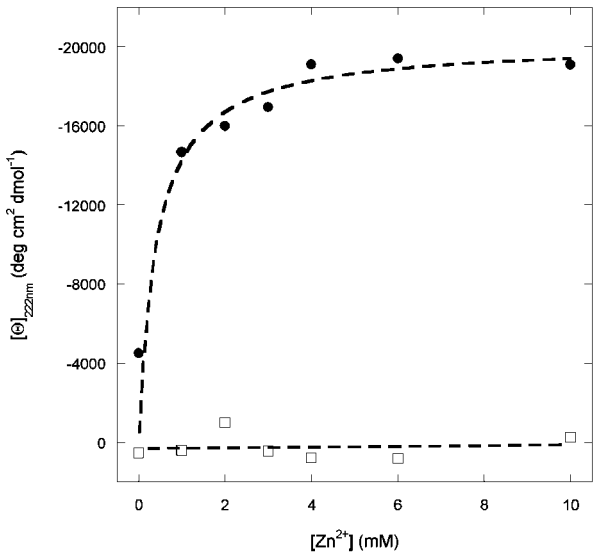

Figure 3. Mean residue ellipticity at 222 nm versus concentration of Zn^{2+} for JR2E (●) and JR2ECref (□). The peptide concentration was kept constant at 200 μM. Lines drawn as a guide for the eye.

and $[\Theta]_{222folded}$ is the helicity of JR2E at pH 4.5.[16] Partial folding of JR2E was also observed upon addition of Fe^{3+}, La^{3+}, Co^{2+}, and Ni^{2+}, but not to the same extent as that for Zn^{2+}. The effect of Ca^{2+} and Mg^{2+} on the secondary structure of JR2E was negligible (Figure 2, inset). Maximum helicity for zinc ion induced folding of JR2E at pH 7 was reached for Zn^{2+} concentrations above 3 mM (Figure 3), corresponding to a 15:1 ratio of zinc to peptide. Quantification of the number of Zn^{2+} bound to each peptide monomer is beyond the scope of this paper. As expected, JR2ECref showed no tendencies to fold at any zinc ion concentration (Figure 3).

The binding of metal ions most probably reduce the charge repulsion between the monomers enough to allow for dimerization and folding as schematically illustrated in Figure 1. The propensity of zinc ions to induce dimerization and folding of JR2EC and JR2E can be explained by the properties of the divalent cation. The completely filled d shell of Zn^{2+} allows a flexible coordination geometry since the ligand field stabilization energy is zero. The borderline acidity of Zn^{2+} (in terms of hard–soft acid–base theory) also means it can interact strongly with a variety of ligand types such as sulfur from cysteine, nitrogen from histidine, and oxygen from water, glutamic acid, and aspartic acid.[29]

The formation of large peptide aggregates due to extended bridging by Zn^{2+}could be ruled out from dynamic light scattering (DLS) experiments. At pH 7.0 in the absence of Zn^{2+} the measured hydrodynamic radius (R_H) of JR2E was 0.7 ± 0.3 nm, which increased to 1.4 ± 0.2 nm as a result of dimerization in the presence of 10 mM Zn^{2+}. No larger objects indicative of peptide aggregation was observed (Supporting Information).

Interaction of Zn^{2+} with Peptide Monomers on Planar Gold. In order to investigate the nature of the interactions of immobilized peptides with Zn^{2+}, JR2EC and JR2ECref were immobilized on planar gold substrates and analyzed using infrared reflection–absorption (RA) spectroscopy, null ellipsometry, and electrochemical impedance spectroscopy before and after exposure to 10 mM Zn^{2+}. The peptides were immobilized on clean gold substrates via the Cys residue in the loop region.

At pH 7 JR2EC is immobilized as a random coil monomer with a film thickness of 13.2 ± 0.3 Å, which corresponds to an approximate surface coverage of 60% of a full monolayer. Here, the measured film thickness was slightly higher than previously reported due to an improved method for cleaning the gold substrates.[30] The film thickness of JR2ECref was not found to be significantly different, 13.0 ± 0.5 Å. A small decrease to 12.5 ± 0.2 Å and 12.6 ± 0.4 Å was observed for both JR2EC and JR2ECref, respectively, after 1 h of incubation in a pH 7.0 solution containing 10 mM Zn^{2+}. The decrease is most probably a consequence of a loss of some loosely associated peptides. Electrochemical impedance spectroscopy (EIS) also confirmed that both peptides form monolayers with similar properties regarding organization and surface coverage, with a rather high double layer capacitance (5–10 μF/cm^2) and a relatively low monolayer resistance (<300 kΩ) indicating that both peptides form thin and unordered films, which easily can be penetrated by ions and water. The impedance spectra also indicate that both peptides respond to the presence of Zn^{2+} in a similar manner (Supporting Information).

Infrared reflection–absorption spectra were recorded for both JR2EC and JR2ECref before and after addition of Zn^{2+} (Figure 4A). The peptides were immobilized as monomers from a buffered pH 7 loading solution. The obtained spectra were strikingly similar with comparable amide I and II intensities and positions, both before and after addition of zinc, indicating that both peptide monomers are bound to the surface and interact with Zn^{2+} in a similar fashion. The similarities in the spectra also indicate that no lateral dimerization and folding occur between JR2EC monomers immobilized on the same surface upon exposure to zinc. The JR2EC amide I and II peaks were found at 1669 and 1542 cm^{-1}, respectively. After a 1 h incubation in a pH 7.0 buffer solution containing 10 mM Zn^{2+}, the amide II peak was slightly shifted to 1540 cm^{-1} while the amide I was unchanged. The amide I to II peak intensity ratio increased from 1.1 to 1.4. A similar trend was observed for JR2ECref, with amide I and II found at 1672 and 1543 cm^{-1}, respectively, before addition of Zn^{2+}. After a 1 h incubation in a buffer solution at pH 7 containing 10 mM Zn^{2+} the amide II peak in the JR2ECref spectrum was slightly red-shifted to 1540 cm^{-1} while the amide I was unchanged. Interestingly, the amide I to II ratio was slightly higher for JR2ECref than for JR2EC both before (1.4) and after (1.6) addition of Zn^{2+}. The most prominent changes in the spectra after zinc treatment did however occur in the region in-between the amide I and II bands, clearly seen in the difference spectra calculated by subtracting the spectra before, from the spectra after addition of zinc (Figure 4B). The amide I and II bands overlap with several of the vibrational modes of the carboxyl groups mainly found in Glu and Asp. The *C*=O stretching vibrations of protonated and uncoordinated carboxylic acids are generally seen at 1750–1700 cm^{-1}, whereas the stretching vibrations of unprotonated and coordinated carboxylic acids give rise to bands near 1650–1590 cm^{-1}. The negative peak in the difference spectra at 1725 cm^{-1} is the result of a decrease in protonated and/or uncoordinated carboxyl groups after addition of Zn^{2+}. A strong positive band at 1606 cm^{-1} and a slightly broader band close to 1416 cm^{-1} are assigned to the asymmetric and symmetric *C*=O carboxylate

(29) Berg, J. M.; Shi, Y. G. *Science* **1996**, *271*, 1081–1085.

(30) Enander, K.; Aili, D.; Baltzer, L.; Lundstrom, I.; Liedberg, B. *Langmuir* **2005**, *21*, 2480–2487.

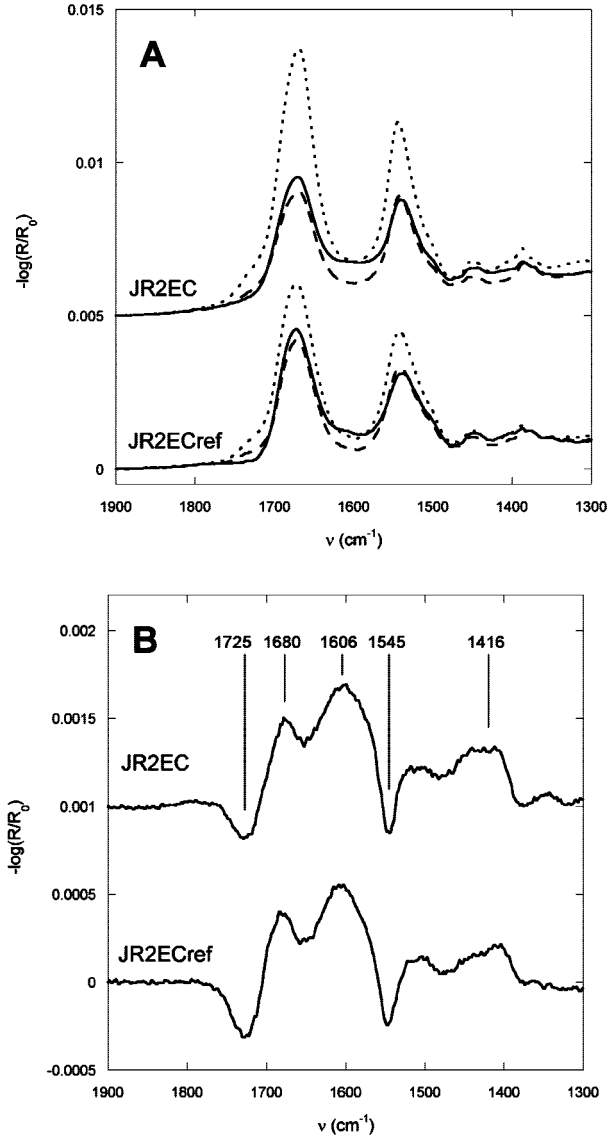

Figure 4. (A) Infrared reflection–absorption spectra of the amide I and II region of JR2EC (top) and JR2ECref (bottom) immobilized on planar gold substrates. (- - -) in the absence of Zn^{2+}, (—) after a 60 min incubation in a 10 mM Zn^{2+} solution at pH 7.0, and (••••••••) when immobilized in the presence of 10 mM Zn^{2+}. (B) Difference spectra of polypeptide coated planar gold substrates showing the change due to binding of Zn^{2+} by the peptide monomers, calculated by subtracting the spectrum before zinc treatment from the spectrum recorded after zinc treatment. JR2EC (top) and JR2ECref (bottom).

stretching vibrations, respectively. As the pH was kept constant the increase in intensity of these peaks suggests Zn^{2+} coordinates to carboxylic acids. The binding of Zn^{2+} to carboxylate groups has previously been observed using IR spectroscopy for a number of organic compounds.[31,32] The acidic Glu and Asp residues are very abundant in the primary structure of JR2E and JR2EC (10 out of 42 amino acids), in particular on the faces of the helices that control dimerization, i.e., in the b and e positions in the heptad repeat. For both JR2EC and JR2ECref the intensity increase of the amide I is seen as a peak at 1680–1688 cm^{-1} in the difference spectra, while the intensity

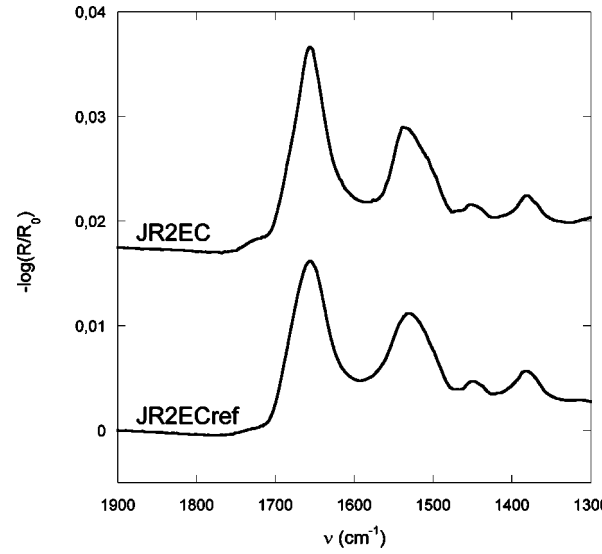

Figure 5. Transmission FT-IR spectra of the amide I and II region of gold nanoparticles functionalized with JR2EC (top) and JR2ECref (bottom) and dried on a CaF_2 window.

decrease of the amide II upon zinc binding results in a dip at 1545 cm^{-1}, indicating that the molecular organization (hydrogen bonding) on the surface is slightly perturbed upon coordination of Zn^{2+}.

Folding on Planar Gold. When immobilized in the presence of 10 mM Zn^{2+}, the ellipsometric thickness increased for both JR2EC and JR2ECref to 21 ± 0.5 Å and 16.3 ± 0.3 Å, respectively. The thickness of the JR2EC monolayer corresponds very well to what has previously been observed when immobilizing the homodimerized and folded peptide (22 Å).[30] The increase in thickness of the JR2ECref film is most probably due to a lowering of the electrostatic repulsion between the peptides during the assembly, which allows for a slightly higher coverage. An increase in the amide I and II intensities was observed for both peptides (Figure 4A) but was particularly pronounced for JR2EC. Both the absolute intensities and the amide I and II intensity ratio of JR2EC are in good agreement with previously reported spectra of homodimerized and folded JR2EC immobilized from acidic loading solutions.[30] The higher peak intensities compared to when immobilized in the absence of Zn^{2+} indicate a significant increase in the amount of adsorbed material, consistent with the ellipsometry data. Only small shifts in amide I and II peak positions were seen, which is also consistent with previously reported data on JR2EC immobilized at acidic conditions. For both peptides, the amide I peak position was unchanged, while the amide II appeared at 1544 cm^{-1} for JR2EC and at 1543 cm^{-1} for JR2ECref, respectively. While the amide I and II ratio of JR2ECref was almost unaltered, a significant increase from 1.1 to 1.5 was observed for JR2EC suggesting an altered and more nativelike conformation[30] when immobilized in the presence of zinc.

Peptide Functionalization of Gold Nanoparticles. Gold nanoparticles with an average diameter of ~13 nm were prepared by reduction of gold chloride with sodium citrate in aqueous solution.[33] JR2EC and JR2ECref were immobilized on the particles by incubating the as-prepared particles in a 100 μM polypeptide solution overnight. Excess peptide molecules were removed by repeated centrifugations reducing the concentration

(31) Tang, L. G.; Hon, D. N. S. *J. Appl. Polym. Sci.* **2001**, *79*, 1476–1485.
(32) Sweeny, D. M.; Curran, C.; Quagliano, J. V. *J. Am. Chem. Soc.* **1955**, *77*, 5508.
(33) Frens, G. *Nature (London) Phys. Sci.* **1973**, *241*, 20–22.

of unbound peptides to less than 0.5 nM. The particles were resuspended in 30 mM Bis-Tris pH 7 after each centrifugation step.

The collective electron oscillations, or localized surface plasmon resonance (LSPR), in gold nanoparticles give rise to a strong extinction band in the visible spectra as described by Mie theory.[34] The resonance wavelength and bandwidth are dependent on the particle size and shape, the refractive index of the surrounding medium, and the temperature.[10,35] Capping of gold nanoparticles by a layer of organic molecules results in a small shift in the LSPR peak position, and the intensity is due to the change in refractive index close to the particle surface. Particle aggregation, on the other hand, results in a massive red shift of the LSPR peak position as well as peak broadening, caused by the near-field coupling between adjacent particles. The magnitude of the red shift is highly dependent on the interparticle distance. The smaller the distance, the larger the resulting red shift.[36,37]

A small shift in the LSPR peak, from 519−520 nm to 523–524 nm, was seen after peptide functionalization. This shift is most probably caused by the change in refractive index in the vicinity of the particle surface upon immobilization of the peptides, but the change of buffer and alterations in particle size distribution as a result of the repeated centrifugations may also contribute.[38] The peptide-capped particles were extremely stable in Bis-Tris buffer at pH 7 and could be stored for more than 12 months without showing any tendency of aggregation, whereas unmodified particles aggregated rapidly and irreversibly upon transfer to Bis-Tris buffer. To further confirm the presence of peptides on the particle surface, IR transmission spectra of solution cast films of peptide-modified particles on CaF_2 windows were recorded (Figure 5). In order to avoid disturbing signals from the buffer, two additional centrifugations where the buffer was exchanged by water (MilliQ 18.2 MΩ cm) were performed. The particles were less stable in water due to the lower ionic strength, and some aggregation occurred. Evaporation of the solvent on the CaF_2 window also gave rise to further particle aggregation. The spectra of the JR2EC and JR2ECref modified particles were, as expected, similar having pronounced amide I and II peaks at 1657 and 1531 cm^{-1} for JR2EC, and 1656 and 1532 cm^{-1} for JR2ECref, and comparable to isotropic spectra of JR2E.[30] The amide I to II ratios were 1.7 and 1.4 for JR2EC and JR2ECref, respectively. The higher ratio for JR2EC may indicate a difference in secondary structure since partial folding of JR2EC can not be excluded as a result of particle aggregation upon drying. No clearly visible bands that could be attributed to other compounds, such as citrate or Bis-Tris, could be seen. Interestingly, the amide I band of the peptides immobilized on planar surfaces was significantly blue-shifted as compared to when immobilized on nanoparticles. Large blue shifts of the amide I peak, ∼13–17 cm^{-1}, have previously been observed when comparing RA spectra of JR2EC with the isotropic spectra of JR2E.[30] A blue shift of the amide I peak (∼20–40 cm^{-1}) also has been reported in a number of earlier studies of proteins adsorbed on metal and metal oxide surfaces,[39,40] and is suggested to result from either alterations in the secondary structure induced by protein−surface interactions or optical effects.[41,42] The optical effects in RA spectra introduce peak shifts toward higher frequencies and are especially pronounced for high-intensity peaks.[41,42] The curvature of nanoparticles may have an effect on the conformation of adsorbed species.[43,44] The smaller the particle radius, the larger the volume of the conical segment that can be occupied by the adsorbed molecules, which allows for a more flexible conformation as compared to when immobilized on planar gold surfaces where the space available for the peptide chain has a cylindrical geometry. The larger the particles, the smaller the effect, and on 13 nm particles the curvature is not expected to be high enough to have any significant impact on the peptide conformation.[44] In addition, the surface coverage as measured on planar substrates is quite low, which will reduce the influence of the surface curvature on the structure of the immobilized peptides. No substrate induced structural differences are therefore to be expected when comparing peptides immobilized on particles to those immobilized on planar surfaces. Thus, it seems reasonable to conclude that the observed blue shifts in the RA spectra of JR2EC and JR2ECref mainly are caused by optical effects.[40,41]

Folding Induced Nanoparticle Aggregation. The stability of nanoparticles, in general, is mainly governed by the balance between attractive van der Waals forces and a repulsive electrostatic force as described by Derjaguin−Landau−Verwey−Overbeek (DLVO) theory.[45] The electrostatic repulsion is the result of overlapping, similarly charged, double layers formed by ions in solution associated or loosely bound to ions or polyelectrolytes adsorbed on the particle surface, whereas the largest contribution to the attractive van der Waals forces originates from London−van der Waal dispersion forces.[46] In DLVO theory the total interaction energy is expressed as the sum of the electrostatic and van der Waals forces. This theory has further been extended to also account for steric forces induced by polymeric or other large bulky molecules bound to the particle surface where the dominant contribution to the repulsive force is a result of the confinement of the configurational entropy of the adsorbed species. In addition, hydrophobic and hydration interactions, among others, contribute to deviations from DLVO behavior.[47] The stability of JR2EC and JR2ECref functionalized gold nanoparticles can mainly be explained by the high net charge of the peptides which effectively stabilizes the dispersions at most pH values. However, in a narrow pH interval ($3.5 < pH < 5$) around the peptide isoelectric point ($pI_{calculated} = 4.56$) the loss of charge causes both JR2EC and JR2ECref functionalized particles to aggregate reversibly which allows for JR2EC monomers immobilized on

(34) Mie, G. *Ann. Phys.* **1908**, *25*, 377–445.
(35) Kelly, K. L.; Coronado, E.; Zhao, L. L.; Schatz, G. C. *J. Phys. Chem. B* **2003**, *107*, 668–677.
(36) Kreibig, U.; Vollmer, M. *Optical Properties of Metal Clusters;* Springer: New York, 1995.
(37) Lazarides, A. A.; Schatz, G. C. *J. Phys. Chem. B* **2000**, *104*, 460–467.
(38) Storhoff, J. J.; Elghanian, R.; Mucic, R. C.; Mirkin, C. A.; Letsinger, R. L. *J. Am. Chem. Soc.* **1998**, *120*, 1959–1964.
(39) Liedberg, B.; Ivarsson, B.; Lundstrom, I. *J. Biochem. Biophys. Methods* **1984**, *9*, 233.
(40) Liedberg, B.; Ivarsson, B.; Hegg, P. O.; Lundstrom, I. *J. Colloid Interface Sci.* **1986**, *114*, 386–397.
(41) Allara, D. L.; Baca, A.; Pryde, C. A. *Macromolecules* **1978**, *11*, 1215–1220.
(42) Ihs, A.; Liedberg, B.; Uvdal, K.; Tornkvist, C.; Bodo, P.; Lundstrom, I. *J. Colloid Interface Sci.* **1990**, *140*, 192–206.
(43) Mandal, H. S.; Kraatz, H. B. *J. Am. Chem. Soc.* **2007**, *129*, 6356-+.
(44) Weeraman, C.; Yatawara, A. K.; Bordenyuk, A. N.; Benderskii, A. V. *J. Am. Chem. Soc.* **2006**, *128*, 14244–14245.
(45) Israelachvili, J. N. *Intermolecular and Surface Forces*; Academic Press: London, 1992.
(46) Glomm, W. R. *J. Disper. Sci. Technol.* **2005**, *26*, 389–414.
(47) Birdi, K. S. *Handbook of Surface and Colloid Chemistry*; CRC Press: Boca Raton, FL, 2003.

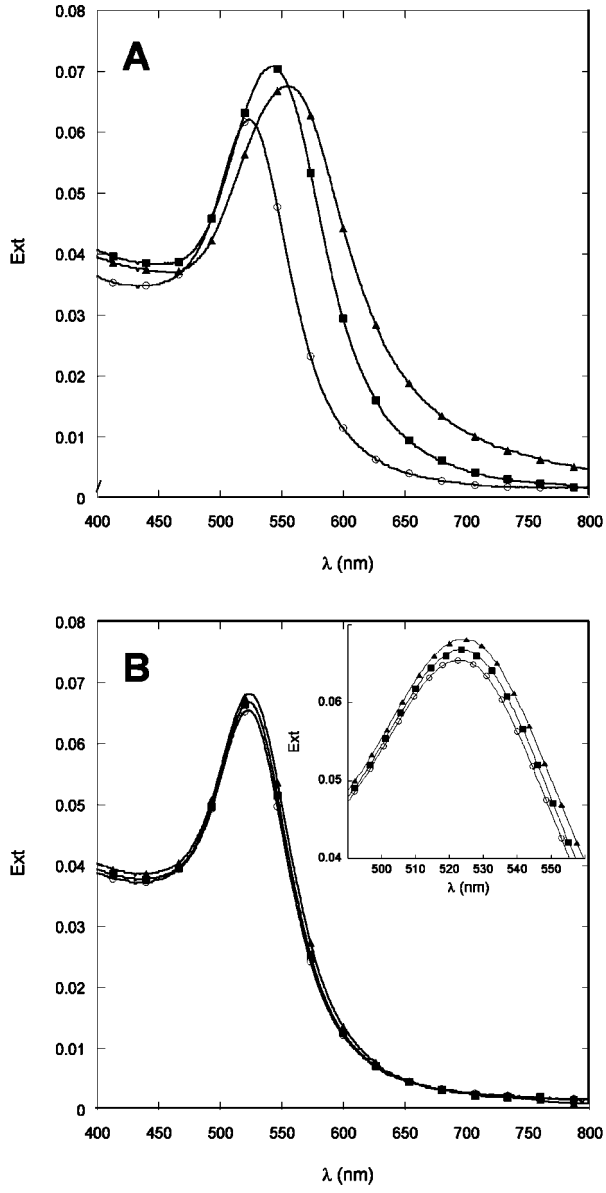

Figure 6. UV–vis spectra of JR2EC (A) and JR2ECref (B) functionalized gold nanoparticles in 30 mM Bis-Tris buffer pH 7. (○) No zinc added, (■) 1 min after addition of 10 mM Zn^{2+}, and (▲) 30 min after addition of 10 mM Zn^{2+}. Inset: The small shift in the LSPR peak position and intensity of JR2ECref functionalized particles is consistent with a small change in refractive index due to binding of Zn^{2+}.

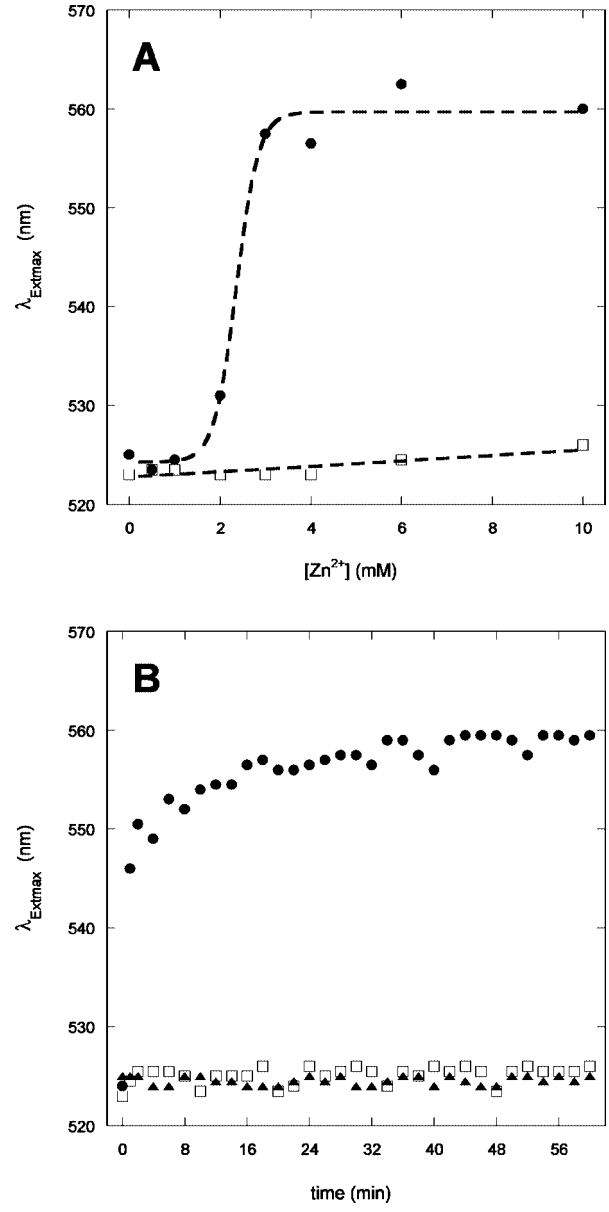

Figure 7. (A) Wavelength of maximum extinction (λ_{Extmax}) of gold particles functionalized with JR2EC (▲) and JR2ECref (■) versus zinc ion concentration after 60 min incubation. Lines drawn as a guide for the eye. B: Change in λ_{Extmax} as a function of time of gold particles functionalized with JR2EC in 10 mM Zn^{2+} (●) and in 10 mM Ca^{2+} (▲), and particles functionalized with JR2ECref in (■) 10 mM Zn^{2+} at pH 7.

neighboring particles to interact, dimerize, and fold. This is an example of aggregation induced folding.[16]

Massive aggregation of JR2EC functionalized particles could also be induced at neutral pH by the addition of zinc ions (Figure 6A). The binding of Zn^{2+} to JR2EC immobilized on gold nanoparticles resulted in rapid aggregation, seen as an almost immediate red shift of the LSPR peak from 523 to 545 nm. The spectrum was further red-shifted during the following minutes before reaching an equilibrium value close to 560 nm. No aggregation of JR2EC functionalized particles occurred for Zn^{2+} concentrations below 2 mM (Figure 7A) or in the presence of citrate, which forms a chelate with Zn^{2+}[48] (data not shown). JR2ECref functionalized particles, on the other hand, displayed only very small changes in the LSPR peak in the presence of 10 mM Zn^{2+} (Figure 6B). A slight increase in intensity and an ~2 nm red shift of the LSPR peak was observed, indicating a change in the refractive index close to the particle surface as a result of binding of Zn^{2+} by the immobilized peptide monomers and the suggested subsequent alteration in molecular organization on the surface. As was discussed above, JR2EC and JR2ECref monomers immobilized on planar gold respond to zinc ions in a similar manner indicating that a loss of charge repulsion is not the major cause of aggregation of JR2EC coated particles. The binding of zinc ions to the JR2EC monomers may however reduce the stability of the particles enough to allow for more short-range forces to become important, such as those involved in dimerization and folding. The ability of JR2EC to dimerize and fold in the presence of Zn^{2+} in solution and the aggregation of only JR2EC functionalized particles upon addition of zinc strongly indicate that aggregation is a conse-

(48) Happe, J. A. *J. Am. Chem. Soc.* **1973**, *95*, 6232–6237.

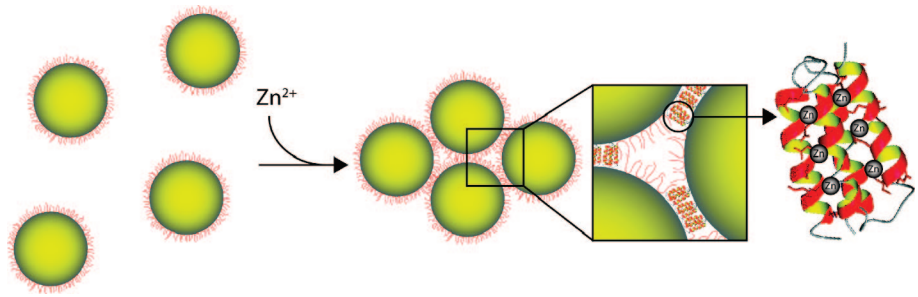

Figure 8. The binding of Zn^{2+} by JR2EC immobilized on gold nanoparticles induces dimerization and folding between peptides located on separate particles resulting in particle aggregation. Removal of the zinc ions by EDTA completely disrupts the aggregates.

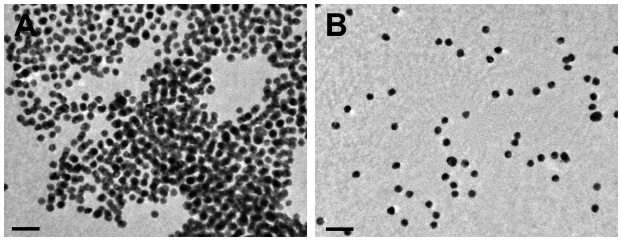

Figure 9. Representative electron micrographs of peptide-decorated nanoparticles incubated with 10 mM Zn^{2+} at pH 7 and dried on carbon coated TEM grids. (A) JR2EC-functionalized particles. (B) JR2ECref-functionalized particles. Scale bar 50 nm.

quence of dimerization and folding between immobilized peptides as schematically illustrated in Figure 8. The importance of folding was further confirmed by the addition of Ca^{2+} to JR2EC functionalized particles. Calcium ions did not induce folding of JR2E in solution, and UV–vis extinction spectra of JR2EC decorated particles dispersed in a pH 7 buffer containing 10 mM Ca^{2+} consequently showed no tendencies of aggregation (Figure 7B), confirming that the particles do not aggregate as a result of an unspecific ion effect. Lateral dimerization between peptides immobilized on the same particle would be sterically impossible and does not occur on planar gold as was shown by IR spectroscopy, which strongly suggests that the dimerization and subsequent folding upon addition of zinc ions takes place between peptides immobilized on different particles. DLS data of JR2E (Supporting Information) also showed that zinc ions did not cause any unspecific bridging between dimerized peptides that in addition to folding could contribute to particle aggregation. Furthermore, TEM micrographs confirmed that JR2ECref functionalized particles were well dispersed even after incubation in a 10 mM Zn^{2+} solution and dried on carbon coated TEM grids, whereas JR2EC functionalized particles showed few, if any, nonaggregated particles after incubation with 10 mM Zn^{2+} (Figure 9). The size of the aggregates spanned from quite small, consisting of tens of particles, to very large. Addition of an excess (15 mM) of ethylenediaminetetraacetic acid (EDTA) to the aggregated particles completely returned the particles to the dispersed state (Figure 10). EDTA is a strong zinc chelator and consequently removes the Zn^{2+} bound to the peptides, which in turn disrupts the dimerization and therefore also the aggregates, resulting in a blue shift of the plasmon peak from ~560 nm back to the initial position at 524 nm. The reversibility of the system was further confirmed by again increasing the concentration of free zinc ions in the same suspension to ~10 mM which brought the LSPR peak back to ~560 nm, followed by an additional injection of EDTA (20 mM) to completely return the LSPR peak to 524 nm (Figure 10B). The decrease in

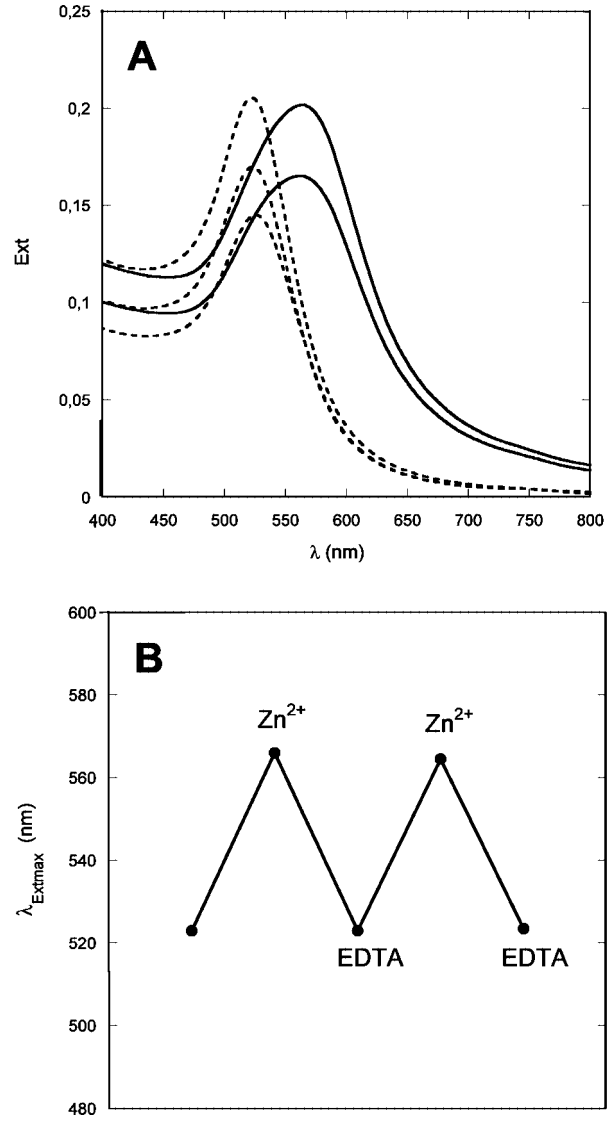

Figure 10. (A) Folding induced aggregation of JR2EC functionalized gold nanoparticles can be repeatedly reversed by subsequent additions of Zn^{2+} and EDTA. (- - -) Extinction before addition of Zn^{2+} or after addition of EDTA and (—) after addition of Zn^{2+}. (B) λ_{Extmax} in the presence of Zn^{2+} and EDTA. Complexation of the Zn^{2+} by an excess of EDTA brings λ_{Extmax} back to 524 nm, whereas an excess of Zn^{2+} causes aggregation.

peak intensity in Figure 10A is a result of the dilution of the particles upon the sequential addition of zinc and EDTA. The dilution alone was, however, not enough to disrupt the aggregates (data not shown).

These findings show that polypeptides with controllable dimerization and folding properties can be used for tuning the assembly of nanoparticles. Folding-induced assembly of nanoparticles is a novel and highly interesting strategy for nanoengineering and allows for new ways of designing and realizing functional composite materials and devices. This study is also a natural extension of our previous work on aggregation induced folding. The chemical and structural diversity and robustness of synthetic polypeptides make them ideal molecular building blocks for the creation of a self-assembling nanoscale Lego. Studies aiming at adding more pieces to this Lego are currently in progress.

Conclusions

We have demonstrated that dimerization and folding of a *de novo* designed synthetic polypeptide immobilized on gold nanoparticles can be utilized to control, and to a certain extent tune, the assembly of the particles. The peptide was designed to fold into a four-helix bundle consisting of two helix–loop–helix monomers upon exposure to Zn^{2+}. When immobilized on gold nanoparticles, addition of zinc ions causes aggregation as an effect of dimerization between peptides immobilized on separate particles. As verified by experiments on planar gold surfaces, the zinc ions coordinate to carboxylic acid groups on Glu and Asp residues, which mainly are located on the faces of the peptide that control dimerization. A reference peptide with the same primary sequence but without the folding ability was utilized to assess the contribution of folding to particle aggregation and for ruling out other effects that could have an influence on particle stability, such as loss of charge repulsion or bridging flocculation. The aggregation of particles could be completely and repeatedly reversed by removal of the zinc ions using EDTA.

Protein folding is a very complex process that is the result of a large number of concerted inter- and intramolecular interactions. The possibility to assemble nanoparticles utilizing these specific and biologically inspired interactions in a controlled and reversible manner provides a highly interesting route for nanoengineering and for the design of new types of composite materials and devices. The optical and chemical properties of gold nanoparticles also provide an interesting tool for a deeper and more fundamental understanding of biomolecular interactions at interfaces.

Acknowledgment. During this study D.A. was enrolled in the graduate school Forum Scientium and in the research programmes Biomimetic Materials Science and NanoSense financed by the Swedish Foundation for Strategic Research (SSF). Financial support from the Swedish Research Council (VR) is also gratefully acknowledged.

Supporting Information Available: DLS data and data analysis of JR2E at pH 7 in the absence and presence of Zn^{2+}. Impedance spectra and equivalent circuit analysis of JR2EC and JR2ECref immobilized on planar gold substrates. This material is available free of charge via the Internet at http://pubs.acs.org.

JA711330F